ELSEVIER

Journal of Organometallic Chemistry 490 (1995) 83–88

Journal of Organometallic Chemistry

$M(CO)_4$ (M = Mo or W) complexes of 2,6-bis(methylthiomethyl)pyridine (L^1) and 2,6-bis(*p*-tolylthiomethyl)pyridine (L^2): a dynamic NMR study

Edward W. Abel, Elizabeth S. Blackwall, Michel L. Creber, Peter J. Heard, Keith G. Orrell *

Department of Chemistry, University of Exeter, Devon EX4 4QD, UK

Received 7 July 1994

Abstract

The hybrid S/N/S donor ligands 2,6-bis(methylthiomethyl)pyridine (L^1) and 2,6-bis(*p*-tolylthiomethyl)pyridine (L^2) react with the $[M(CO)_5(THF)]$ (M = Mo or W) compounds to form complexes of general formula $[M(CO)_4L]$ (M = Mo, L = L^2; M = W, L = L^1 or L^2), where both L^1 and L^2 act in a S/N bidentate chelate fashion. In solution, these complexes undergo three fluxional processes, viz. inversion at the coordinated S atom, S^1–S^2 switching, and combined inversion and S^1–S^2 switching, leading to an interconversion of the four possible permutational isomers. Energy barriers for all three processes have been evaluated by standard one-dimensional band-shape analysis techniques. The mechanism of the S^1–S^2 switch is discussed.

Keywords: Molybdenum; Tungsten; Fluxionality; Nuclear magnetic resonance

1. Introduction

Transition metal complexes of ligands which possess a redundant donor group are recognised as potentially fluxional species. The stereochemical non-rigidity associated with the bidentate chelate bonding mode of 2,2′:6′,2″-terpyridine (terpy) has been the subject of much recent interest [1–7], and is illustrative of this type of latent fluxionality. In such complexes, the pendant pyridyl ring undergoes an exchange with the equivalent coordinated ring in a 1,4-metallotropic shift process. Similarly, the ligands 2,6-bis(methylthiomethyl)pyridine (L^1) and 2,6-bis(*p*-tolylthiomethyl)pyridine (L^2) can also bond to transition metal moieties in a bidentate chelate fashion, and have been shown to undergo analogous fluxional rearrangements [8,9].

We describe here the fluxionality associated with the Group VI tetracarbonyl complexes of 2,6-bis(methylthiomethyl)pyridine and 2,6-bis(*p*-tolylthiomethyl) pyridine, viz. $[M(CO)_4L]$ (M = Mo, L = L^2; M = W, L = L^1 or L^2). In these complexes, the hybrid S/N/S ligands act in a five-membered S/N bidentate chelate fashion, and the pendant S donor group is shown to exchange with the coordinated S group. Two further fluxional processes have also been identified, viz. inversion at the coordinated S donor atom and combined inversion and S^1–S^2 switching.

2. Experimental details

2.1. General

All manipulations were performed under dry, oxygen-free nitrogen, by standard Schlenk techniques [10]. All solvents were dried [11], and degassed prior to use. The ligands 2,6-bis(methylthiomethyl)pyridine [8,12] and 2,6-bis(*p*-tolylthiomethyl)pyridine [13] were synthesised by literature methods and identified by their NMR spectra. The complexes $[M(CO)_5(THF)]$ (M = Mo or W) were also prepared by standard procedures [14] and characterised by IR spectroscopy.

Infrared spectra were recorded as CH_2Cl_2 solutions on a Perkin-Elmer model 881 spectrometer using matched CaF_2 solution cells. Elemental analyses were carried out by Butterworth Laboratories Ltd., Teddington, Middlesex.

^1H NMR spectra were recorded as $(CDCl_2)_2$ solutions on either a Bruker AM250 or AC300 Fourier transform spectrometer operating at 250.13 MHz or 300.13 MHz, respectively. Chemical shifts are quoted relative to tetramethylsilane as an internal standard.

* Corresponding author.

SSDI 0022-328X(94)05192-5

NMR probe temperatures were controlled using a standard B-VT 1000 unit, with the calibration being checked periodically against a Comark digital thermometer; probe temperatures are considered accurate to within ±1°C. NMR band shapes were analysed using the authors' version of the DNMR3 program [15]. The activation parameters were obtained from a least-squares fitting of the Eyring and Arrhenius plots using the THERMO program previously described [16].

2.2. Synthesis of complexes

The complexes $[M(CO)_4L]$ (M = Mo, L = L^2; M = W, L = L^1 or L^2) were prepared by the addition of a THF solution of $[M(CO)_5L]$ (M = Mo or W) to a stirred THF solution of the appropriate ligand. The procedure for $[M(CO)_4L^1]$ is given below as an illustrative example.

$[M(CO)_5(THF)]$ (2.56 mmol in 60 cm^3 of THF) was added dropwise to a stirred solution of 2,6-bis(methylthiomethyl)pyridine (0.5 g, 2.56 mmol) in 20 cm^3 of THF. The reactants were heated at 50°C for ca. 2 h, and then the solvent was concentrated to dryness in vacuo. The crude product was purified by recrystallisation from a mixture of CH_2Cl_2 and *n*-hexane (1:2 v/v) at 0°C. Yield; 0.33 g, 66%.

Synthetic and analytical data for all three complexes, $[M(CO)_4L]$ (M = Mo, L = L^2; M = W, L = L^1 or L^2), are reported in Table 1.

3. Results and discussion

The complexes $[M(CO)_4L]$ (M = Mo, L = L^2; M = W, L = L^1 or L^2) were obtained in moderate yield as described (vide supra). Attempts to isolate pure samples of the complexes $[Mo(CO)_4L^1]$ and $[Cr(CO)_4L]$ (L = L^1 or L^2) were unsuccessful. This appears to be because of their instability in solution. This suggestion is supported by the significant levels of decomposition observed for the three complexes studied, as evidenced by their variable-temperature ^1H NMR spectra (vide infra). The NMR signals of the decomposition products were sharp at all temperatures, and did not interfere with the subsequent dynamic studies. Furthermore, the poor analytical data obtained for the complexes $[M(CO)_4L]$ (M = Mo, L = L^2; M = W, L = L^1) (Table 1) suggest that these complexes are also unstable in the solid state.

Table 1
Synthetic and analytical data for the complexes $[M(CO)_4L]$ (M = W, L = L^1 or L^2; M = Mo, L = L^2)

Complex	Reaction time (h)	Yield [a] (%)	ν(CO) [b] (cm^{-1})	Analytical data (%)	
				Found	Calculated
$[W(CO)_4L^1]$	2	66	2010	C 28.50	31.53
			1905vs,b [c]	H 1.78	2.65
			1843	N 2.72	2.83
$[W(CO)_4L^2]$	4	70	2020	C 45.48	46.38
			1900vs,b [c]	H 3.29	3.27
			1846	N 2.17	2.16
$[Mo(CO)_4L^2]$	2	57	2011	d	
			1911vs,b [c]	d	
			1852	d	

[a] Yield quoted relative to $[M(CO)_6]$.
[b] Infrared data; recorded as CH_2Cl_2 solutions; vs = very strong, b = broad.
[c] Composite band resulting from overlap of both the A_1 and B_1 stretching modes.
[d] Unreliable analyses because of decomposition of the complex $[Mo(CO)_4L^2]$.

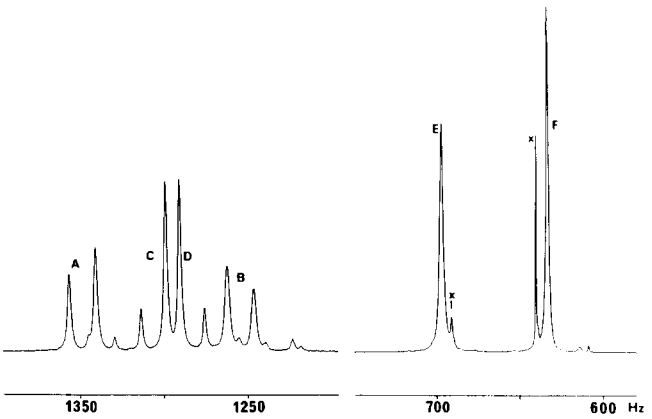

Fig. 1. The 250 MHz ^1H NMR spectrum of $[W(CO)_4L^1]$ in $(CDCl_2)_2$ at 273 K showing the ligand methyl and methylene signals. Labelling refers to Fig. 2. Impurity signals denoted X.

The IR spectra of the complexes $[M(CO)_4L]$ (M = Mo, L = L^2; M = W, L = L^1 or L^2) showed fewer than the number of C≡O stretching bands expected for a *cis*-$M(CO)_4$ moiety [17]. However, the broad band at ca. 1900–1910 cm^{-1} is assumed to result from overlap of one of the A_1 modes with the B_1 mode [18].

^1H NMR spectra were recorded on freshly prepared samples of all three complexes, and confirmed the bidentate chelate-bonding modes of the ligands, L^1 and L^2, suggested by the analytical data. The ambient temperature (303 K) ^1H NMR spectra of the complexes $[M(CO)_4L]$ (M = Mo, L = L^2; M = W, L = L^1 or L^2) showed exchange-broadened signals. However, on cooling, the lines sharpened and well-resolved spectra were obtained. The spectra of all three complexes were very similar, and the case of $[W(CO)_4L^1]$ will serve to illustrate the analysis of the solution-state stereodynamics. The ^1H NMR spectrum of $[W(CO)_4L^1]$ at 273 K (Fig. 1) comprised three regions: (i) the ligand–methyl region (ca. δ = 2.1–2.3); (ii) the ligand–methylene region (ca. δ = 4.2–4.6); and (iii) the aromatic region (ca. δ = 7.2–7.9).

The ligand–methyl region consisted of two signals in a 1:1 intensity ratio. The higher frequency band was

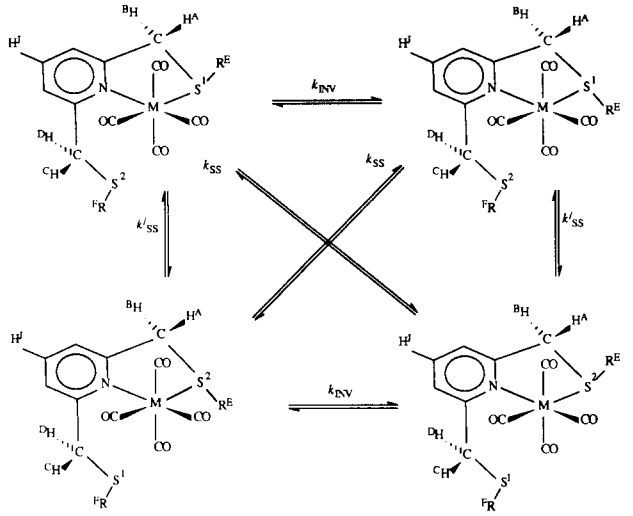

Fig. 2. Four permutational isomers of the complexes $[M(CO)_4L]$ ($L = L^1$ or L^2) showing their interconversions resulting from inversion of the coordinated S atom, fluxional S^1–S^2 switching of the ligand, and combined S inversion and S^1–S^2 switching.

assigned to the methyl group of the chelate ring (Me_E, Fig. 2), because it would be expected to be deshielded by virtue of its proximity to the metal-coordinated S atom. The lower frequency signal was thus attributed to the pendant ligand–methyl group.

The ligand–methylene region comprised two sets of AB quartets in a 1:1 intensity ratio. One set was widely spaced ($\Delta\delta = 0.31$), and assigned to the hydrogen atoms of the chelate ring (H_A and H_B, Fig. 2) because they would be expected to be more sensitive to the orientation of the coordinated S substituent group. The second AB quartet ($\Delta\delta = 0.06$) was therefore assigned to the pendant methylene hydrogen atoms, H_C and H_D. The aromatic region was not fully resolved; however, a sharp triplet assignable to H_J of the central pyridyl ring was resolved, and its chemical shift and coupling constant measured precisely (Table 2). Table

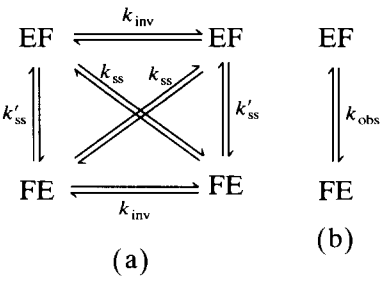

Scheme 1.

2 contains the ^1H NMR data for all three complexes $[M(CO)_4L]$ (M = Mo, $L = L^2$; M = W, $L = L^1$ or L^2).

Four permutational isomers of the complexes are depicted in Fig. 2. These are associated with the three rate processes occurring, viz. inversion at the coordinated S atom, a fluxional process which switches the metal coordination from one S atom to the other (S^1–S^2 switching) and a process involving combined inversion and S^1–S^2 switching. The equatorial plane of symmetry of the $M(CO)_4$ moiety renders all four structures chemically indistinguishable, but exchanges between them can be followed from the consequent NMR magnetisation transfers.

When $(CDCl_2)_2$ solutions of all three complexes were warmed, these magnetisation transfers caused changes in the aromatic, methylene and methyl regions of the ^1H NMR spectra. Attention was paid to the changes in the methylene and methyl regions. The ligand–methylene signals are sensitive to all three rate processes, whereas the ligand–methyl signals are totally insensitive to the pyramidal S inversion, because no transfer of magnetisation takes place as a result of this process. The ligand–methyl signals were therefore used to obtain a separate evaluation of the rates of the S^1–S^2 switching process. The dynamic scheme (1a) can be simplified to scheme (1b), because the pathways

Table 2
^1H NMR data [a] for the complexes $[M(CO)_4L]$ (M = W, $L = L^1$ or L^2; Mo, $L = L^2$)

Complex	Temperature (K)	$\delta(p\text{-}C_6H_4\text{-}CH_3)$	$\delta(S\text{-}CH_3)$	$\delta(-CH_2-)$ [b,c]	$\delta(Py\text{-}H_J)$ [b]
$[W(CO)_4L^1]$	273	–	2.32 2.11	4.49 (15.86) (A) 4.34 (14.70) (C) 4.28 (14.70) (D) 4.18 (15.86) (B)	7.79 (7.90)
$[W(CO)_4L^2]$	273	1.66 1.63	–	4.19 (14.79) (A) 4.05 (16.03) (C) 3.93 (14.79) (B) 3.81 (16.03) (D)	6.93 (7.74)
$[Mo(CO)_4L^2]$	243	2.30 2.27	–	4.75 (14.36) (A) 4.57 ((14.36) (B) 4.44 (12.96) (C) 4.40 (14.70) (D)	7.59 (6.58)

[a] Spectra recorded in $(CDCl_2)_2$ solution; chemical shifts quoted relative to $SiMe_4$ as an internal standard.
[b] $^2J_{HH}$/Hz in parentheses.
[c] See Fig. 2 for labelling.

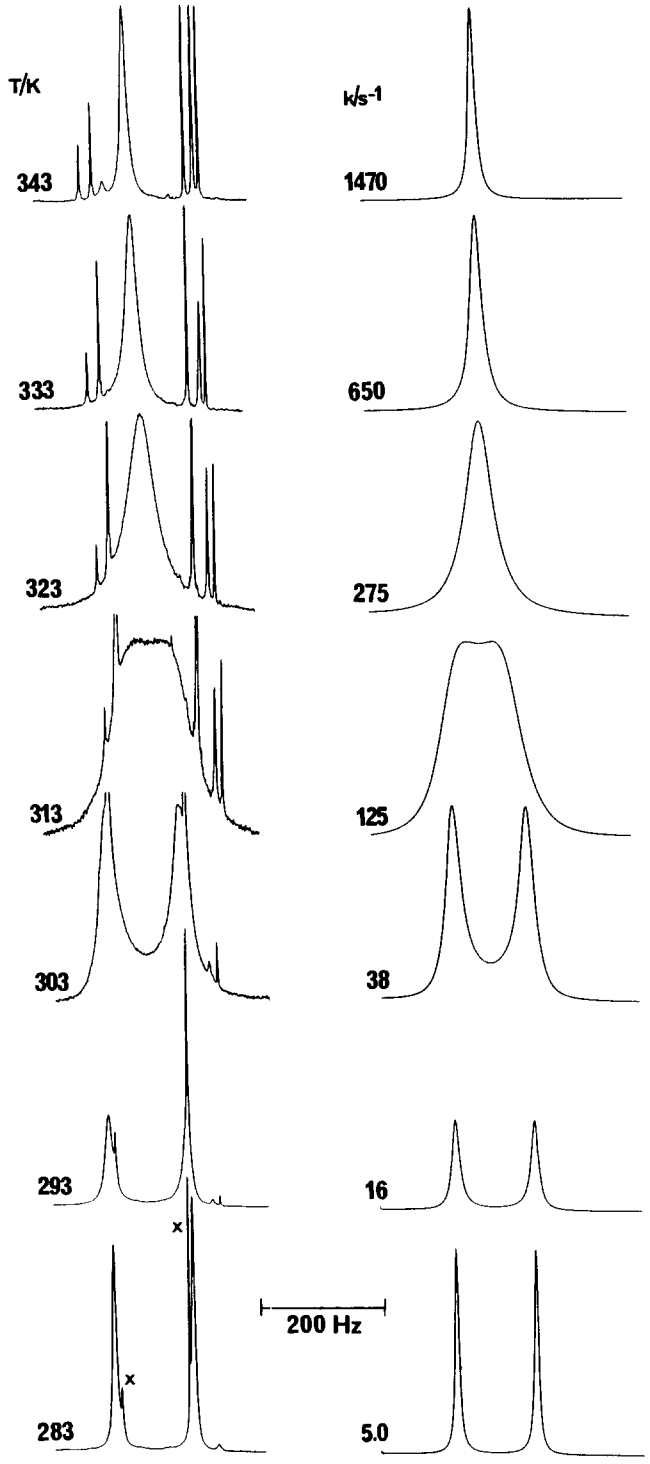

Fig. 3. Variable temperature ^{1}H NMR spectra of the ligand methyl signals of $[W(CO)_4L^1]$, with computer-simulated spectra and "best-fit" rate constants, k_{obs}, shown alongside. Two impurity signals depicted by X.

defined by k_{ss} and k'_{ss} (Fig. 2) cannot be distinguished. The ligand–methyl signals were therefore simulated to derive values of the rate constant k_{obs}, and the fittings for the complex $[W(CO)_4L^1]$ are shown in Fig. 3. "Best-fit" rate constants are given in Table 3.

Table 3
"Best-fit" first-order rate constants (s^{-1}) for the three rate processes in the complex $[W(CO)_4(L^1)]$

Temperature (K)	k_{inv}	k_{ss}	k'_{ss}
283	≈ 0	5.0	≈ 0
293	2.5	16.0	≈ 0
303	7.5	38.0	3.5
313	33.0	125	9.0
323	78.0	275	27.0
333	190	650	69.0
343	500	1470	220

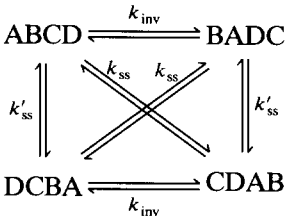

Scheme 2.

In the ligand–methylene region the ^{1}H NMR signals are sensitive to all three rate processes, as shown in Scheme (2).Because there are no spin–spin couplings between the pendant and chelate methylene groups, Scheme (2) reduces to a pair of degenerate two-spin systems, Scheme (3).

It was not possible to fit the ligand–methylene spectra to a unique set of three independent rate constants, and so the k_{obs} rate constants for the S^1–S^2 switching process were used to reduce the number of independent variables. Two cases were tested: (i) when $k_{obs} = k_{ss}$ (i.e. $k_{ss} \gg k'_{ss}$) and (ii) $k_{obs} = 2k_{ss}$ (i.e. $k_{ss} = k'_{ss}$). These cases were chosen to examine whether the probability of S^1–S^2 switching occurring without apparent inversion at the coordinated S atom was considerably greater than or equal to the probability of the combined S^1–S^2 switching and inversion process. Only the first case gave good agreement between experimental and computer simulated line shapes (Fig. 4). However, these fittings showed that k'_{ss} values were not totally negligible, but approximately 10% of the k_{ss} values at any given temperature (Table 3). Thus it appears that the S^1–S^2 fluxion proceeds preferentially without apparent inversion at the coordinated S atom. The nature of the transition state for the combined process is not known precisely, as it is unclear whether the k'_{ss} path-

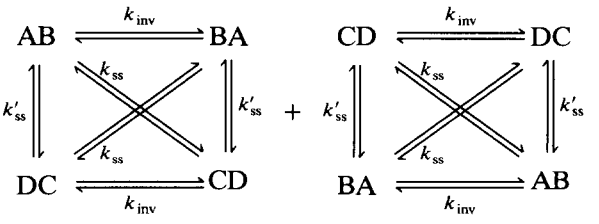

Scheme 3.

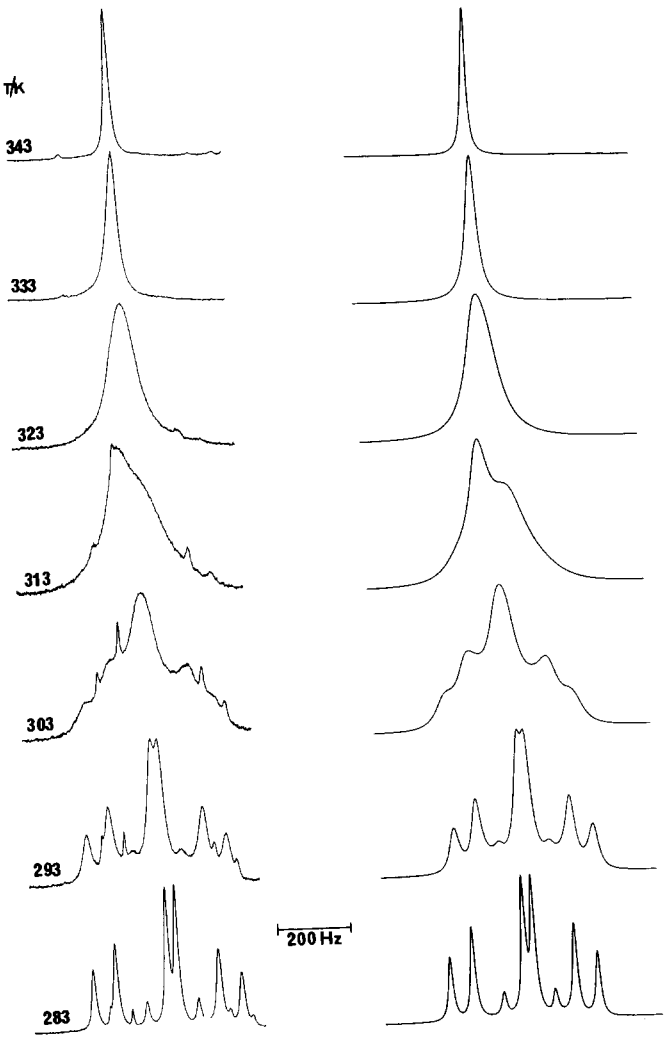

Fig. 4. Variable temperature ^{1}H NMR spectra of the ligand methylene signals of $[W(CO)_4L^1]$, with computer-simulated spectra based on Scheme 3 (see text) shown alongside. "Best-fit" rate constants are reported in Table 3.

way refers to a synchronous or consecutive S^1–S^2 switch and S inversion. In the consecutive process, the S inversion may be seen not as a conventional pyramidal inversion via a planar transition state, but simply as an indication of the different orientations of the S-substituent (Me or *p*-tolyl) in the initial and final structures.

The variable-temperature spectra revealed signs of considerable decomposition of the complexes $[M(CO)_4L]$ (M = Mo, L = L^2; M = W, L = L^1 or L^2) (e.g. Figs. 3 and 4). However the analyses of the dynamic NMR line shapes were not adversely affected. The Eyring and Arrhenius activation parameters calculated from the rate data are presented in Table 4.

Examination of the $\Delta G^{\ddagger}$ (298.15 K) values obtained for the complexes $[M(CO)_4L]$ (M = Mo, L = L^2; M = W, L = L^1 or L^2) (Table 4) reveals several points of interest.

(i) For all three processes, viz. pyramidal sulfur inversion, S^1–S^2 switching, and combined inversion and S^1–S^2 switching, the magnitudes of $\Delta G^{\ddagger}$ of the tetracarbonyltungsten(0) complexes $[W(CO)_4L]$ (L = L^1 or L^2) are greater than those of the tetracarbonylmolybdenum(0) complex $[Mo(CO)_4(L^2)]$. This ordering of $\Delta G^{\ddagger}$ values with respect to the metal moiety, i.e. $W^0 > Mo^0$, is in accord with the trends previously noted for molybdenum and tungsten sulfur-ligand complexes [19].

(ii) The magnitudes of $\Delta G^{\ddagger}$ for the S^1–S^2 switching process in the tetracarbonyltungsten(0) complexes $[W(CO)_4L]$ (L = L^1 or L^2) increase as the mass/size of the sulfur substituent increases, i.e. $\Delta G^{\ddagger}[W(CO)_4L^2] > \Delta G^{\ddagger}[W(CO)_4(L^1)]$. The greater magnitude of $\Delta G^{\ddagger}$ of the 2,6-bis(*p*-tolylthiomethyl)pyridine complex, $[W(CO)_4(L^2)]$, may be related either to a slight stabilisation of the ground state or a slight destabilisation of the transition state. The former seems more probable because the complex $[Mo(CO)_4(L^1)]$ (vide supra) and related platinum(IV) complexes $[PtXMe_3L^1]$ (X = Cl, Br or I) proved too unstable to isolate [9].

(iii) Comparison of the $\Delta G^{\ddagger}$ (298.15 K) values for the S^1–S^2 switching process obtained for the complexes $[M(CO)_4L]$(M = Mo, L = L^2; M = W, L = L^1 or

Table 4
Activation parameters [a] for the complexes $[M(CO)_4L]$ (M = W, L = L^1 or L^2; M = Mo, L = L^2)

Complex	Process	E_a (kJ mol^{-1})	$\log_{10} A$ (s^{-1})	$\Delta H^{\ddagger}$ (kJ mol^{-1})	$\Delta S^{\ddagger}$ (J K^{-1} mol^{-1})	$\Delta G^{\ddagger}$ (kJ mol^{-1})
$[W(CO)_4L^1]$	inversion	88.7(2.8)	16.2(0.5)	86.0(2.8)	56.7(8.8)	69.1(0.2)
	S^1–S^2 switch [b]	76.7(0.7)	14.9(0.1)	74.0(0.7)	30.5(2.2)	64.9(0.1)
	inv-ss	89.0(3.3)	15.9(0.5)	86.4(3.3)	49.5(10.2)	71.6(0.2)
$[W(CO)_4L^2]$	inversion	[d]	[d]	[d]	[d]	[d]
	S^1–S^2 switch [b]	84.2(7.5)	15.4(1.3)	81.6(7.5)	40.4(24.1)	69.6(0.3)
	inv-ss	[d]	[d]	[d]	[d]	[d]
$[Mo(CO)_4L^2]$	inversion	72.8(5.8)	14.5(1.1)	70.4(5.8)	23.7(20.1)	63.3(0.3)
	S^1–S^2 switch [b]	85.0(2.1)	17.8(0.4)	82.5(2.1)	87.2(7.0)	56.4(0.1)
	inv-ss	64 [c]	11.7(3.2)	58 [c]	−29.0(61.8)	67.1(0.3)

[a] Errors quoted in parentheses; $\Delta G^{\ddagger}$ quoted at 298.15 K.
[b] Values obtained by simulation of the ligand–methyl region of the ^{1}H NMR spectra.
[c] Error uncertain.
[d] Not evaluated.

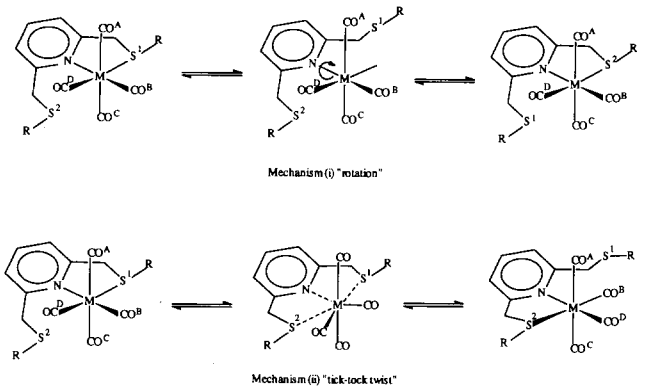

Fig. 5. The two possible mechanisms for the S^1–S^2 switching process in the complexes $[M(CO)_4L]$ ($L = L^1$ or L^2).

L^2) with those for the analogous halogenotricarbonylrhenium(I) [8] and halogenotrimethylplatinum(IV) [9] complexes reveals the following trend with respect to the metal moiety: $Re^I > W^0 > Pt^{IV} > Mo^0$. This is different to the trends observed previously in the analogous 2,2′:6′,2″-terpyridine complexes [1], viz. $Re^I > Pt^{IV} > W^0 > Mo^0$, and results from a large increase in the magnitude of $\Delta G^{\ddagger}$ (298.15 K) for the W^0 complexes $\{\Delta(\Delta G^{\ddagger}) \approx 11$ kJ mol$^{-1}\}$ on changing the ligand from 2,2′ : 6′,2″-terpyridine to either 2,6-bis(*p*-tolylthiomethyl)pyridine or 2,6-bis(methylthiomethyl) pyridine. This increase is not easy to rationalise, and presumably arises from a number of factors, such as the change in the ligand "bite-size" and the effects of the hybrid sulfur donor atoms.

Two possible mechanisms have been proposed for the S^1–S^2 switching process [8,9]. These are depicted in Fig. 5. Mechanism (i) involves the loosening of the metal–sulfur bond, followed by a 180° rotation about the metal–nitrogen bond. Mechanism (ii) involves the simultaneous loosening of both the metal–sulfur and the metal–nitrogen bonds, followed by a twist through the S–M–N bond angle (ca. 90°). In principle, it is possible to distinguish between these two mechanisms by virtue of their different effects on the equatorial metal substituents (i.e. those *trans* to the M–S and M–N bonds) (Fig. 5). Thus dynamic ^{13}C NMR studies on the M–CO signals of the complexes $[M(CO)_4L]$ ($M = Mo$, $L = L^2$; $M = W$, $L = L^1$ or L^2) should have provided an unambiguous method for the determination of the mechanism. However, the poor solubility and instability of these complexes prevented the acquisition of good quality ^{13}C NMR spectra, and the mechanism could not be proven conclusively.

However, two-dimensional ^1H NMR exchange studies on the platinum–methyl signals of the complex $[PtBrMe_3L^2]$ [9] *did* enable the mechanism of the S^1–S^2 switching process to be established. In that case, mechanism (ii) was found to be operative. By analogy, it seems probable that the same "tick-tock twist" mechanism is operating in the present $[M(CO)_4L]$ complexes.

Acknowledgements

We are grateful to the SERC and the University of Exeter, respectively, for research studentships to E.S.B. and P.J.H.

References

[1] E.W. Abel, N.J. Long, K.G. Orrell, A.G. Osborne, H.M. Pain and V. Šik, *J. Chem. Soc., Chem. Commun.*, (1992) 303.
[2] E.R. Civitello, P.S. Dragovich, T.P. Karpishin, S.G. Novick, G. Bierach, S.J. O'Connell and T.D. Westmoreland, *Inorg. Chem.*, *32* (1993) 237.
[3] E.W. Abel, V.S. Dimitrov, N.J. Long, K.G. Orrell, A.G. Osborne, V. Šik, M.B. Hursthouse and M.A. Mazid, *J. Chem. Soc., Dalton Trans.*, (1993) 291.
[4] E.W. Abel, V.S. Dimitrov, N.J. Long, K.G. Orrell, A.G. Osborne, H.M. Pain, V. Šik, M.B. Hursthouse and M.A. Mazid, *J. Chem. Soc., Dalton Trans.*, (1993) 597.
[5] H.M. Pain, *Ph.D. Thesis*, University of Exeter, 1993.
[6] E.W. Abel, K.G. Orrell, A.G. Osborne, H.M. Pain and V. Šik, *J. Chem. Soc., Dalton Trans.*, (1994) 111.
[7] E.W. Abel, K.G. Orrell, A.G. Osborne, H.M. Pain, V. Šik, M.B. Hursthouse and K.M.A. Malik, *J. Chem. Soc., Dalton Trans.*, (1994) 3441.
[8] E.W. Abel, D. Ellis and K.G. Orrell, *J. Chem. Soc., Dalton Trans.*, (1992) 2243.
[9] E.W. Abel, P.J. Heard, K.G. Orrell, M.B. Hursthouse and M.A. Mazid, *J. Chem. Soc., Dalton Trans.*, (1993) 3795.
[10] D.F. Shriver, *Manipulation of Air-Sensitive Compounds*, McGraw-Hill, New York, 1969.
[11] D.D. Perrin and W.L.F. Armarego, *Purification of Laboratory Chemicals*, Pergamon, Oxford, 1985.
[12] D. Ellis, *Ph.D. Thesis*, University of Exeter, 1989.
[13] D. Parker, J-M Lehn and J. Rimmer, *J. Chem. Soc., Dalton Trans.*, (1985) 1517.
[14] T.E. MacKenzie, *Ph.D. Thesis*, University of Exeter, 1983.
[15] G. Binsch and D.A. Kleier, *DNMR3, Program* 165, *Quantum Chem. Prog. Exchange*, Indiana University, USA, 1970.
[16] V. Šik, *Ph.D. Thesis*, University of Exeter, 1979.
[17] L.E. Orgel, *Inorg. Chem.*, *1* (1962) 25.
[18] C.S. Kraihanzel and F.A. Cotton, *Inorg. Chem.*, *2* (1963) 533.
[19] E.W. Abel, S.K. Bhargava and K.G. Orrell, *Prog. Inorg. Chem.*, *32* (1984) 1.